

Detection of Defects in Additively Manufactured Metals Using Thermal Tomography



Alexander Heifetz, Dmitry Shribak, Zoe L. Fisher, and William Cleary

Abstract Quality control of additively manufactured (AM) metallic structures is essential prior to deployment of these structures in a nuclear reactor. We investigate the limits of detection of sub-surface porosity defects in AM stainless steel 316L using thermal tomography nondestructive evaluation method. Thermal tomography reconstructs spatial thermal effusivity of the structure from time-dependent surface temperature measurements of flash thermography. Our studies are based on computer simulations of heat transfer through solids using COMSOL software suit. Using the model of layered media, in which defect in a solid is represented with a layer of un-sintered metallic powder with appropriate thermophysical parameters, we obtain depth profile of thermal effusivity for the structure. Computer simulations indicate that at 1 mm depth, layers of 50 μm thickness are detectable in SS316L.

Keywords Additive manufacturing · Nondestructive evaluation · Thermal tomography

Introduction

Additive manufacturing (AM) is an emerging method for cost-efficient production of low-volume custom and unique parts with minimal supply-chain dependence. In particular, AM potentially provides a cost-saving option for replacing aging nuclear reactor parts and reducing costs for new construction of advanced reactors [1]. Metals of interest for passive structures in nuclear applications typically include

A. Heifetz (✉) · D. Shribak · Z. L. Fisher
Nuclear Science and Engineering Division, Argonne National Laboratory, Argonne, IL, USA
e-mail: aheifetz@anl.gov

Z. L. Fisher
Nuclear Science and Engineering Department, Massachusetts Institute of Technology, Cambridge, MA, USA

W. Cleary
Fuel Fabrication Facility, Westinghouse Electric Company, Columbia, SC, USA

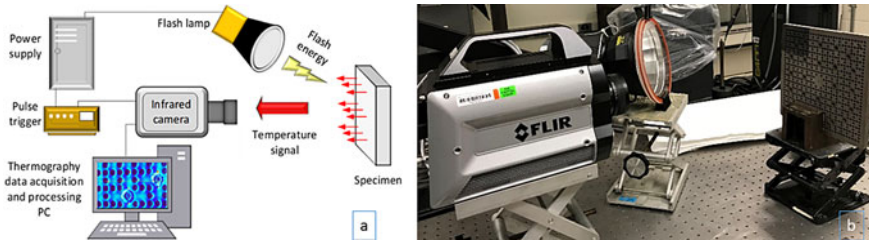


Fig. 1 **a** Schematics of pulsed thermal tomography system. **b** Laboratory setup. (Color figure online)

high-strength corrosion-resistant stainless steel and nickel super alloys. Because of high strength, shape forming of these metals into complex geometry structures is not trivial. AM of such metals is currently based on laser powder-bed fusion (LPBF). Because of the intrinsic features of LPBF, material defects such as porosity and anisotropy can appear in the metallic structure [2, 3]. A pore is potentially a seed for crack formation in the structure due to thermal and mechanical stresses in nuclear reactor. Quality control (QC) in AM involves detection of material flaws in real time during manufacturing, and nondestructive evaluation (NDE) of the structure after manufacturing. Currently, there exist limited options for nondestructive examination (NDE) of AM structures either during or post-manufacturing. Deployment of high-resolution NDE systems, such as X-ray tomography, is limited by spatial constraints of the metal 3D printer, large size, and complex shapes with lack of rotational symmetry of the AM parts. Contact NDE techniques, such as ultrasound, face challenges because AM structures have rough surfaces which affect probe coupling. In addition, NDE methods such as ultrasound require time-consuming point-by-point raster scanning of specimens.

As a solution to NDE of AM structures, we are developing pulsed thermal tomography (PTT) algorithms for 3D imaging and material flaw detection [4, 5]. The method is non-contact and scalable to arbitrary structure size. A schematic depiction of the PTT setup is shown in Fig. 1. The method consists of illuminating material with white light flash lamp, which rapidly deposits heat on the material surface. Heat transfer then takes place from the heated surface to the interior of the sample, resulting in a continuous decrease of the surface temperature. A megapixel fast frame infrared (IR) camera records thermograms, time-resolved images of surface temperature distribution $T(x, y, t)$. Thermal tomography obtains reconstruction of 3D spatial effusivity $e(x, y, z)$ from the data stack of thermography images.

Thermal Tomography Principles

The reconstruction algorithm of thermal tomography obtains apparent spatial effusivity $e(x, y, z)$ from time-dependent surface temperature $T(x, y, t)$ measurements of flash thermography. The reconstruction model assumes that heat propagation is

one-dimensional along the z -coordinate. This assumption is strictly valid for uniform planar structures. However, approximate solutions can be obtained for locally planar structures. Detailed study of non-planar structures is outside the scope of this paper. For 1D heat diffusion,

$$\frac{\partial T}{\partial t} = \alpha \frac{\partial^2 T}{\partial z^2}, \tag{1}$$

where z is the depth coordinate, x and y are coordinates in the transverse plane, and α is thermal diffusivity defined as

$$\alpha = k/\rho c. \tag{2}$$

Here, k is thermal conductivity, ρ is density, and c is specific heat. The reconstructed $e(z)$ at the location (x, y) in the plane is obtained only from the surface temperature transient $T(t)$ measured at the location (x, y) . The algorithm starts with the assumption that the medium can be treated as semi-infinite. The analytic solution for semi-infinite slabs is given as [2–4]

$$T(z, t) = \frac{Q}{\sqrt{\rho c k \pi t}} \exp\left(-\frac{z^2}{4\alpha t}\right), \quad 0 \leq z \leq \infty, \tag{3}$$

where Q is the instantaneously deposited surface thermal energy density (J/m^2). Thermal effusivity, which is a measure of how the material exchanges thermal energy with its surroundings, is defined as

$$e = \sqrt{\rho c k}. \tag{4}$$

Using Eqs. (3) and (4), one can express observed or apparent time-dependent effusivity of the medium as

$$e(t) = \frac{Q}{T(z = 0, t)\sqrt{\pi t}}. \tag{5}$$

Using the characteristic relationship between time and depth [5–7]

$$z = \sqrt{\pi \alpha t}. \tag{6}$$

And relating temporal effusivities $e(z)$ and $e(t)$ are related through a convolution integral, where $1/z$ is the transfer function [5–7]

$$e(t) = \int_0^z z^{-1} e(\zeta) d\zeta. \tag{7}$$

We obtain the final equation for apparent effusivity as

$$e(z) = z \frac{2Q}{\pi \sqrt{\alpha}} \frac{d}{dt} \left(\frac{1}{T(t)} \right) \Big|_{t=z^2/\pi\alpha} \quad (8)$$

This shows that spatial reconstruction of apparent effusivity $e(z)$ is given as a product of depth function z and time derivative of the inverse of surface temperature evaluated at time t corresponding to depth z according to Eq. (6). Information obtained from thermal tomography is relative because Q is usually not known. In principle, relative information can be converted to absolute scale through calibration. However, for estimation of geometrical parameters and detecting material flaws, relative effusivity reconstruction in non-dimensional units is sufficient.

Parametric Studies of Apparent Effusivity Reconstruction with COMSOL Computer Simulations of Heat Transfer

To obtain estimates of thermal tomography sensitivity to defects in LPBF, we reconstruct apparent effusivity from data generated with COMSOL computer simulations of heat transfer in a layered metallic structure. The structure modeled in COMSOL is a stainless steel disc with $R = 30$ cm radius and $L = 5$ mm thickness. Diffusion of heat in a plate with such geometry (transverse dimensions are much larger than the thickness) closely resembles the case of an infinite plate of finite thickness. For the solid media in the structure, we used stainless steel 316L thermophysical parameters $\rho = 7954$ kg/m³, $k = 13.96$ W/m*K, $c = 499.07$ J/kg [8]. For modeling the amplitude of defect layer, we linearly scaled the thermophysical parameters as $\eta\rho$, ηc and ηk , where ρ , c and k are those of the solid metal, and the scaling parameter values are in the range $\eta = 0.7$ – 0.9 . The range of scaling parameter values was chosen to correspond to that of the filling factor of un-sintered metallic powder. According to random close packing (RCP) model, packing density of mono-dispersed spheres is 0.65 [9], but size distribution and non-spherical shapes of powders may result in higher packing density [10]. Working in normalized units, we set $\rho = c = k = 1$ for solid medium, so that $e_{\text{solid}} = 1$. While density and heat capacity typically scale linearly with powder filling factor, scaling of thermal conductivity is potentially nonlinear. Therefore, this study provides information about parametric dependence of effusivity reconstruction, where a hypothetical defect does not exactly correspond to a physical powder model.

The defect was introduced into the structure as a layer of metallic material with lower thermophysical parameters than those of the host solid plate. In LPBF, heat diffusion is likely to result in smooth transitions from solid metal to defect. The defect was introduced into COMSOL grid as a subtracted Gaussian with the mean of μ and standard deviation σ . Thus, in normalized units, the defect actual effusivity is modeled as

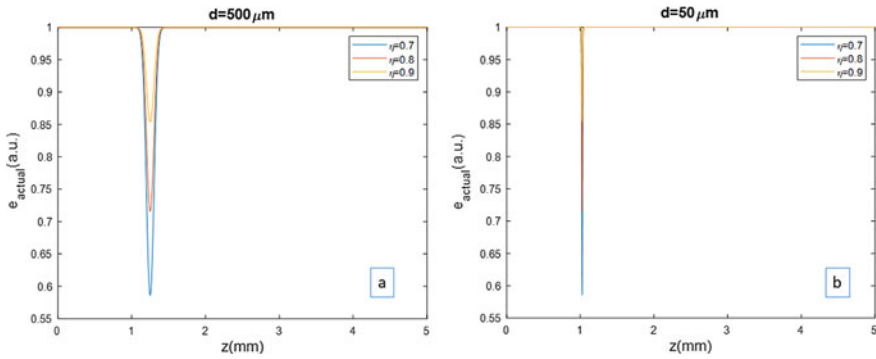


Fig. 2 Actual effusivities in normalized units for $L = 5$ mm plate with a defect layer with equivalent thickness of **a** $d = 500 \mu\text{m}$ and **b** $d = 50 \mu\text{m}$. (Color figure online)

$$e_{actual}(z) = \left(1 - (1 - \eta)e^{-(z-\mu)^2/2\sigma^2}\right)^{3/2} \quad (9)$$

Defects with equivalent width of $d = 500 \mu\text{m}$ and $d = 50 \mu\text{m}$ were considered in COMSOL computer simulations of the layered model. The defects were modeled as subtracted Gaussians with $\mu = 1.25$ mm and $\sigma = 50 \mu\text{m}$, and $\mu = 1.025$ mm and $\sigma = 5 \mu\text{m}$, respectively. Actual effusivities for the two defects are plotted in Figs. 2a and b. The scaling parameter η in both figures is in the range from 0.7 to 0.9.

In COMSOL computer simulations, the plate is initially at room temperature, and the incident heat source is a Gaussian pulse with variance of 0.5 ms. Although the reconstruction model in thermal tomography assumes that heat was deposited instantaneously on the material surface, real flash heat sources have a finite duration time. High intensity flash is usually generated by discharging a capacitor through a white light lamp, with typical capacitor time constant on the order of a few milliseconds (see Fig. 1). Thermal insulating boundary conditions were selected for all plate surfaces. Temperature transients were calculated with 0.1 ms time step for 20 s total problem runtime. Temperature data was exported from COMSOL to perform apparent effusivity reconstruction with algorithm implemented in MATLAB. We observed in COMSOL simulations that the surface temperature of the plate is maximum at the time when the incident Gaussian heat pulse reaches the maximum value. While heat is still applied by the pulse, surface plate temperature begins to decay due to diffusion of heat into the bulk of the plate. This affects the decay rate of the surface temperature. Therefore, when performing effusivity reconstruction, the origin of the surface temperature transient should be chosen such that the heat source has no effect on surface temperature decay. The starting time for the temperature transient used for effusivity reconstruction is 8 ms after the surface temperature reaches the maximum value.

Figure 3a–c shows apparent effusivity reconstructions for scaling parameter $\eta = 0.7, 0.8,$ and $0.9,$ respectively. In each figure, reconstructions are shown for a structure containing a defect with $d = 500 \mu\text{m}$ layer and another structure containing

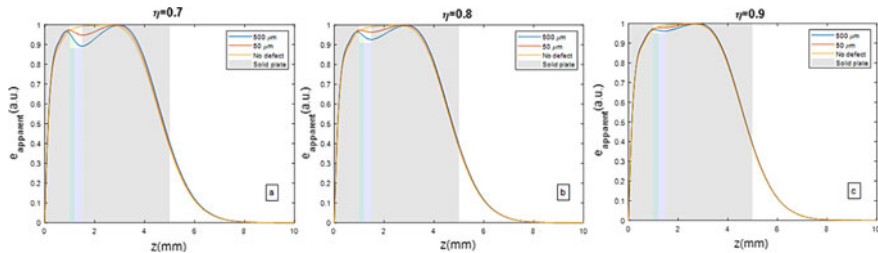


Fig. 3 Apparent effusivity $e(z)$ reconstructions for variable defect thermophysical properties from surface temperature transients produced with COMSOL computer simulations data of heat transfer. The structure has $L = 5$ mm total thickness with Gaussian defect. Thermophysical parameters of the defect layer are scaled as $\eta\rho$, ηc and ηk , where ρ , c and k are those of the SS316L solid metal, and the scaling parameter values are in the range **a** $\eta = 0.7$ **b** $\eta = 0.8$ **c** $\eta = 0.9$. (Color figure online)

$d = 50 \mu\text{m}$ layer. Apparent effusivity reconstruction $e(z)$ is plotted as a normalized variable. In the sketch of the layered structure shown in Fig. 3, the front and back planes are at $z = 0$ and at $z = 5$, respectively. Detection of defect is interpreted as deviation from the effusivity reconstruction for a defect-free solid plate. The defect layer is indicated as $500 \mu\text{m}$ and $50 \mu\text{m}$ -thick stripes overlaid on the solid plate structure colored in gray. The strip is slightly larger than 2σ width of the Gaussian model of the defect. One can observe from Fig. 3 that the reconstruction for a solid plate with no defect (yellow curve) agrees well at the front edge of the plate. However, reconstruction is blurred at the back edge of the plate. As the scaling factor η is decreased, apparent effusivity depth profile curve shows a dip in the spatial region corresponding to the defect. As expected, the dip decreases with increasing value of η .

Quantitative analysis of the data in Fig. 3 is shown in Table 1. Reconstructed effusivity of the defect is obtained by measuring the minimum value at the dip of the effusivity curve. Based on computer simulations for defects located below 1 mm depth, reconstruction of the defect with $500 \mu\text{m}$ thickness offers approximately 10–5% contrast, while reconstruction of the defect with $50 \mu\text{m}$ thickness offers approximately 5–2% contrast relative to solid plate effusivity.

Table 1 Apparent effusivity of defect layer obtained from COMSOL computer simulations

η	Defect apparent effusivity (normalized units)	
	500 μm	50 μm
0.7	0.89	0.95
0.8	0.93	0.96
0.9	0.96	0.98

Conclusion

Our results based on computer simulations of heat transfer in a layered media indicate that detection of defects as small as 50 μm located at 1 mm depth in SS316L can be possible, in principle. Because results are obtained from simulated data with no experimental noise, results based on computer simulations are likely to give the upper bound for detection of material defects with thermal tomography reconstructions of experimental data. In addition, sensitivity threshold of IR camera in detecting temperature differences has to be taken into consideration. Future work will be aimed performing experimental validations of thermal tomography sensitivity with imprinted calibrated defects.

Acknowledgements This project is sponsored by NEET Advanced Methods in Manufacturing (AMM) program. Other contributors include Brian Saboriendo, Thomas Elmer, and Sasan Bakhtiari from Argonne National Laboratory, Boris Khaykovich from MIT Nuclear Laboratory, Gregory Banyay and Leo Carrilho from Westinghouse Electric Company.

References

1. Lou X, Gandy D (2019) Advanced manufacturing for nuclear energy. *JOM* 71:2834–2836
2. Lewandowski JJ, Seifi M (2016) Metal additive manufacturing: a review of mechanical properties. *Ann Rev Mater Res* 46:151–186
3. King WE, Anderson AT, Ferencz RM, Hodge NE, Kamath C, Khairallah SA, Rubenchik AM (2015) Laser powder bed fusion additive manufacturing of metals: physics, computational and materials challenges. *Appl Phys Rev* 2:041304
4. Heifetz A, Shribak D, Liu T, Elmer TW, Kozak P, Bakhtiari S, Khaykovich B, Cleary W (2019) Pulsed thermal tomography nondestructive evaluation of additively manufactured reactor structural materials. *Trans Am Nucl Society* 121(1):589–591
5. Heifetz A, Elmer TW, Sun JG, Liu T, Shribak D, Saboriendo B, Bakhtiari S, Zhang X, Saniie J (2019) “First annual report on pulsed thermal tomography nondestructive evaluation of additively manufactured reactor materials and components,” ANL-19/43
6. Sun JG (2016) Quantitative three-dimensional imaging of heterogeneous materials by thermal tomography. *J Heat Transf* 138:112004
7. Sun JG (2014) Pulsed thermal imaging measurement of thermal properties for thermal barrier coatings based on a multilayer heat transfer model. *J Heat Transfer* 136:081601
8. Kim CS (1975) “Thermophysical properties of stainless steels,” ANL-75-55
9. Jaeger HM, Nagel SR (1992) Physics of granular states. *Science* 255(5051):1523–1531
10. Donev A, Cisse I, Sachs D, Variano EA, Stillinger FH, Connelly R, Torquato S, Chaikin PM (2004) Improving the density of jammed disordered packings using ellipsoids. *Science* 303(5660):990–993